

## Research Article

# *ABC* Fractional Derivative for Varicella-Zoster Virus Using Two-Scale Fractal Dimension Approach with Vaccination

Jirong Yang,<sup>1</sup> Farkhanda Afzal ,<sup>2</sup> and Perpetual Appiah <sup>3</sup>

<sup>1</sup>Shaanxi University of Chinese Medicine, Xiayang, Shaanxi 712046, China

<sup>2</sup>MCS, National University of Sciences and Technology, Islamabad, Pakistan

<sup>3</sup>Department of Mathematics, University of Cape Coast, Ghana

Correspondence should be addressed to Perpetual Appiah; [perpetual.appiah@stu.ucc.edu.gh](mailto:perpetual.appiah@stu.ucc.edu.gh)

Received 26 August 2022; Revised 6 September 2022; Accepted 19 September 2022; Published 14 October 2022

Academic Editor: Muhammad Nadeem

Copyright © 2022 Jirong Yang et al. This is an open access article distributed under the Creative Commons Attribution License, which permits unrestricted use, distribution, and reproduction in any medium, provided the original work is properly cited.

Chickenpox or varicella is an infectious disease caused by the varicella-zoster virus (*VZV*). This virus is the cause of chickenpox (usually a primary infection in the nonimmune host) and herpes zoster. In this paper, a compartmental model for the dynamics of *VZV* transmission with the effect of vaccination is solved using the *ABC* fractional derivative. The possibility of using the fractal dimension as a biomarker to identify different diseases is being investigated. The problem is investigated in two different levels of research using two scale dimensions. To ascertain the existence and uniqueness of the solution, we qualitatively evaluate the model. We have used the Euler method to compute the numerical solution for the system. At the end, we provide the graphical results showing the effectiveness of two-scale dimension and fractional calculus in the current model.

## 1. Introduction

Chickenpox, or varicella, is caused by the varicella-zoster virus (*VZV*), a globally distributed herpes virus [1]. Chickenpox occurs in all countries, killing about 7,000 people annually. This is a common illness in children in temperate countries, ten with them. [2, 3]. The itchy blister rash caused by a chickenpox infection appears for 10 to 21 days and usually lasts about 5 to 10 days. Other signs and symptoms that may appear 1-2 days before the rash appears are fever, decreased appetite, headache, and general malaise. Chickenpox spreads from one individual to another by direct contact with the blisters, saliva, or mucus of an infected individual. The virus can also spread in the air by coughing or sneezing. There are different theories about the origin of the name of this disease. After infection, the skin appeared to have been picked out from the chicken. Another reason is that the rash mimics chickpea seeds. The most usual interpretation is that the disease is a type of “chickenpox” because it is not as severe as smallpox. Chickenpox occurs differently depending on the geographical area. Anyhow, the occurrence of chickenpox in these regions increased between adolescents and

adults [4], which may in part be due to an increase in global tourism and economic migration. In most tropical areas, situation is changed, with 60 percent of the immunized adult population [5]. Previously, the said virus infects almost the whole population, causing significant morbidity and mortality from both primary varicella zoster and reactivation of herpes zoster. The first approved vaccine for varicella was used in 1995 reducing the severity, morbidity, and mortality rate significantly. In 2006, due to the outbreak of illness caused by a single vaccination schedule, the children were recommended to receive their second dose vaccination series. The innovation of the shingles vaccine has also benefited the elders. For those over 60, the Food and Drug Administration approved the use of a shingles vaccination in 2006 that contained high amounts of the primary varicella vaccine’s live attenuated vaccine. Millions of individuals could help prevent the disease caused by the varicella-zoster virus by lowering the prevalence and mortality of shingles and postherpetic neuralgia.

Compared to integer-order calculus, many real-world problems can be better explained when using fractional operators. Fractional calculus is recognized as a promising

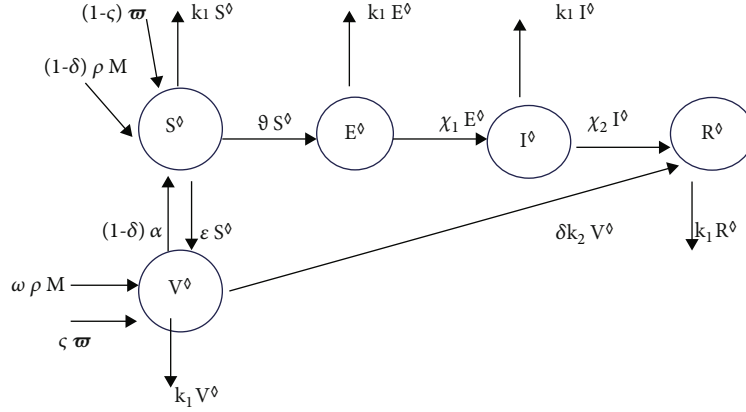


FIGURE 1: Flow diagram of VZV.

mathematical tool for efficiently characterizing historical memories and global correlations of complex dynamical systems, phenomena, or structures. Fractional-order PDEs dominate the majority of models of physical fluid dynamics events, electricity, ecological structure, quantum physics, and many others. Understanding positive integer order  $_{35}$  derivatives and integrals are of great importance for the development of modern theoretical and practical problems of science. Properties of integral, differential operators, and mathematical functions are as follows: gamma, beta, and other special functions where the integral takes the form of convolution, and there are singularities are useful.

Development of fractal theory was formulated by Mandelbrot. The second half of the 20th century generally integrated the work of many other early mathematicians and scientists, opening a new perspective on this goal. Since then, several attempts have been made to interpret the relationship between fractional operators and this new geometry. As the dynamic foundations of fractional calculus and fractal dimensions, fractal theory and FDE theory are rapidly gaining popularity as disciplines around the world.

Physical memory and heredity are clearly defined by fractions. Special functions, elliptic integrals, and elliptic functions are used in various physical systems. Their inclusion in solving nonlinear differential equations is well known. You can examine these functions and integrals using the references. Fractional differential operators are becoming robust, and systematic mathematical tools for studying various scientific and biological events nowadays, for example, childhood disease [14, 16], HIV, coronary heart disease [15], hepatitis C [17], Chikungunya virus [18], and Crimean-Congo hemorrhagic fever (CCHF) [19], can be seen in the references. Fractional-order differential equations, in contrast to integer-order differential equations, can show nonlocal interactions with memory cores in time and space [6, 7].

**1.1. Motivation.** The complexity, validity, implementation, prevention, therapy, and control strategies of mathematical models have been improving. Following the research, the entire population is divided into three categories: susceptible, infectious, and eliminated with lifelong acquired immu-

nity. This approach is known as the SIR model. In real life situations after a time, in the infectious compartment, the individuals, recovered or removed individuals, lose immunity and return to the susceptible compartment. These models are known as SIRS models. Following the same assumptions, the model 2 can be written in the following form [13].

$$\begin{aligned}
 \frac{dS^\circ}{dt} &= (1-\omega)\rho M + (1-\zeta)\varpi + (1-\delta)\alpha \mathcal{V}^\circ - (\vartheta + \kappa_1 + \epsilon)S^\circ, \\
 \frac{d\mathcal{V}^\circ}{dt} &= \omega\rho M + \zeta\varpi + \kappa_1 S^\circ - ((1-\delta)\alpha + \delta\kappa_2 + \epsilon)\mathcal{V}^\circ, \\
 \frac{d\mathcal{E}^\circ}{dt} &= \vartheta S^\circ - (\chi_1 + \epsilon)\mathcal{E}^\circ, \\
 \frac{dI^\circ}{dt} &= \chi_1 \mathcal{E}^\circ - (\chi_2 + \epsilon)\mathcal{I}^\circ, \\
 \frac{d\mathcal{R}^\circ}{dt} &= \chi_2 \mathcal{I}^\circ + (\delta\kappa_2)\mathcal{V}^\circ - \epsilon\mathcal{R}^\circ.
 \end{aligned} \tag{1}$$

Figure 1 shows the block diagram of the model under consideration. It can be seen that susceptible vaccinated classes have direct relationship. And engineering and science fields like biotechnology, medicine, biological processes, artificial intelligence, and space sciences all make extensive use of mathematical modeling of physical systems. Scientists, engineers, and mathematicians are turning to the broad field of mathematical modeling to solve the numerous issues they face. We take into account the Atangana-Baleanu fractional operator in the sense of Caputo to investigate the fractional dynamics of a model under consideration. The utilization of the Atangana-Baleanu partial derivatives is based on their nonlocal characteristics. This operator is better for capturing complex behaviors. Table 1 gives definitions of variables.

## 2. Contribution and Novelty

Mathematical methods are based on the application of some basic principles of fractional differentiation and first-order

TABLE 1: Variables' definitions.

Variables & Parameters	Interpretation
$\mathcal{S}^\circ(t)$	Susceptible individuals
$\mathcal{V}^\circ(t)$	Vaccinated individuals
$\mathcal{E}^\circ(t)$	Exposed individuals
$I^\circ(t)$	Infected individuals
$R^\circ(t)$	Recovered individuals
$\rho$	Per capita birth rate
$\kappa_1$	Natural mortality rate
$\chi_2$	Rate has permanent immunity after recovery
$\omega$	Consistent recruitment rate
$\varsigma$	Vaccinated recruit
$\omega$	Vaccinated infants
$\vartheta$	Rate of first-dose vaccine received by susceptible individuals

interpolation. An analysis is conducted on the existence and uniqueness of the model. According to the interesting attractors obtained in this study, these new fractal-fractional operators may be able to explain new elements of the behavior of these systems rather than fractional derivatives. Some of these properties go beyond the traditional integer-order operators. It is trendy to examine the real life problems using fractional approaches because the fractional derivative covers a broad spectrum of variables as compared to integer order derivatives. Two-scale dimension is a new approach for dealing with the problems involving more than one scale of observation. This paper combines the benefits of fractional derivative and efficacy of two-scale dimension to study a wide spread virus model [24].

This study differs from previous studies on schemes due to the involved new formulation of a two-scale fractal fractional derivative. Atangana and his colleagues first published some of these new derivative theories in 2017. They combine the concepts of fractional and fractal derivatives, taking into account nonlocality, memory, and fractal effects. This model takes into account processes such as power law, fading memory, and crossovers. Note that this article uses a significantly different numerical approach and analysis than [13], which describes the integer ordering problem. It has been shown that the two-scale fractal dimension has a significant impact on the dynamics of the system.

$$\begin{aligned}
 {}_0^{\mathcal{ABC}}\mathcal{D}_t^\nu \mathcal{S}^\circ &= (1 - \omega)\rho M + (1 - \varsigma)\omega + (1 - \delta)\alpha \mathcal{V}^\circ - (\vartheta + \kappa_1 + \epsilon)\mathcal{S}^\circ, \\
 {}_0^{\mathcal{ABC}}\mathcal{D}_t^\nu \mathcal{V}^\circ &= \omega\rho M + \varsigma\omega + \kappa_1\mathcal{S}^\circ - ((1 - \delta)\alpha + \delta\kappa_2 + \kappa_1)\mathcal{V}^\circ, \\
 {}_0^{\mathcal{ABC}}\mathcal{D}_t^\nu \mathcal{E}^\circ &= \vartheta\mathcal{S}^\circ - (\chi_1 + \kappa_1)\mathcal{E}^\circ, \\
 {}_0^{\mathcal{ABC}}\mathcal{D}_t^\nu \mathcal{I}^\circ &= \chi_1\mathcal{E}^\circ - (\chi_2 + \kappa_1)\mathcal{I}^\circ, \\
 {}_0^{\mathcal{ABC}}\mathcal{D}_t^\nu \mathcal{R}^\circ &= \chi_2\mathcal{I}^\circ + (\delta\kappa_2)\mathcal{V}^\circ - \kappa_1\mathcal{R}^\circ.
 \end{aligned}
 \tag{2}$$

*Definition 1.* Let  $\varsigma$  be a function which is continuous in the domain  $(a, b)$  with  $\nu \in (0, 1]$ . The  $\mathcal{ABC}$  fractional derivative is defined as [8]

$${}_0^{\mathcal{ABC}}\mathcal{D}_t^\nu \varsigma(t) = \frac{\mathcal{M}(\nu)}{1 - \nu} \frac{d}{dt} \int_0^t \varsigma(\zeta) E_\nu \left[ \frac{-\nu}{1 - \nu} (t - \zeta)^\nu \right] d\zeta. \tag{3}$$

The normalization constant  $\mathcal{M}(\nu)$  gives  $\mathcal{M}(0) = \mathcal{M}(1) = 1$ .

*Definition 2.* The fractional integral related with the fractional derivative is given as [8, 9]

$${}_0^{\mathcal{ABC}}I_t^\nu \varsigma(t) = \frac{1 - \nu}{\mathcal{M}(\nu)} \varsigma(t) + \frac{\nu}{\mathcal{M}(\nu)\Gamma(\nu)} \int_0^t [(t - \zeta)^{\nu-1}] \varsigma(\zeta) d\zeta. \tag{4}$$

*2.1. ABC Fractional Order Model for  $\mathcal{V}^\circ \mathcal{E}^\circ \mathcal{I}^\circ$ .* Over the last few decades, some researchers and scientists have emphasized fractional calculus and have shown that it is a better tool to study natural events by fractional order than the integer order. Fractional calculus supported the popularity and benefits of fractal modeling. This section explains the adoption of the numerical method for Atangana-Baleanu's fractional differential operator [23]. The iterative expression obtains via  $\mathcal{ABC}$  fractional model to Eq. (2) as follows:

$$\begin{aligned}
 \mathcal{S}^\circ(t) - \mathcal{S}^\circ(0) &= \frac{1 - \nu}{\mathcal{M}(\nu)} [(1 - \omega)\rho M + (1 - \varsigma)\omega + (1 - \delta)\alpha \mathcal{V}^\circ \\
 &\quad - (\vartheta + \kappa_1 + \epsilon)\mathcal{S}^\circ] + \frac{\nu}{\mathcal{M}(\nu)\Gamma(\nu)} \\
 &\quad \cdot \int_0^t [(t - \zeta)^{\nu-1}] [(1 - \omega)\rho M + (1 - \varsigma)\omega \\
 &\quad + (1 - \delta)\alpha \mathcal{V}^\circ - (\vartheta + \kappa_1 + \epsilon)\mathcal{S}^\circ] d\zeta.
 \end{aligned}
 \tag{5}$$

For simplification, we write

$$\Theta_1(t, \mathcal{S}^\circ) = (1 - \omega)\rho M + (1 - \varsigma)\omega + (1 - \delta)\alpha \mathcal{V}^\circ - (\vartheta + \kappa_1 + \epsilon)\mathcal{S}^\circ. \tag{6}$$

### 3. Two-Scale Dimension

Mathematics plays a vital role in the science of measurement. Mathematical models are needed to recognize how powerful dimensional systems are structured and to investigate the results they produce. How about measuring a coastline? In this example, the concept of length is not applicable. Land mass features exist on multiple scales, but there is no clear scale of minimum features to consider when measuring. The smooth and idealized length of the metal rod can be precisely measured with the help of measuring instrument to determine whether the length is less than one value and greater than the other. The accuracy of the true value depends on the accuracy of the instrument. However, improving the measuring instrument does not improve the accuracy of coastline surveying. As with metal rods, there

is no way to give a specific value to the length of the coastline.

The coastline problem applies to the idea of a fractal surface in 3D space where the area of the surface changes with the measurement scale. Many laws of physics are scale-dependent and give scale-dependent results. In these systems, behavior is “scale dependent” and can be assumed to be accompanied by drastic changes in behavior associated with an exclusive regime. Einstein’s theory of relativity made researchers believed that applying the theory of relativity to a similar scale could account for the usage of scale dependence in practical problems, see [10] to study the details of the two-scale transformation.

$$\Delta S = \frac{\Delta t^\nu}{\Gamma(1+\nu)}, \quad (7)$$

where  $\Delta S$  is the smaller scale,  $\Delta t$  is the larger scale, and  $\nu$  is two-scale dimension. Two scales provide a logical explanation in terms of existing fractal calculus theories. This is a modern concept that emphasizes the importance of scale in the examination of practical problem [20, 21]. In [11, 12], the work presented was the source of our motivation. As an illustration of the concepts presented in the aforementioned articles, we will present our own work.

**Theorem 3.**  $\Theta_1$  fulfills the Lipschitz condition and contraction if the following inequality holds:

$$0 \leq (\vartheta + \kappa_1 + \epsilon) < 1. \quad (8)$$

*Proof.* Let  $a = (\vartheta + \kappa_1 + \epsilon)$ . For  $S^\circ$ , we have

$$\begin{aligned} \Theta_1(t, S^\circ) - \Theta_1(t, S_1^\circ) &= -(\vartheta + \kappa_1 + \epsilon)(S^\circ - S_1^\circ(t)) \\ &\leq (\vartheta + \kappa_1 + \epsilon)(S^\circ - S_1^\circ(t)). \end{aligned} \quad (9)$$

□

We get the following result:

$$\Theta_1(t, S^\circ) - \Theta_1(t, S_1^\circ) \leq a(S^\circ(t) - S_1^\circ(t)). \quad (10)$$

Consequently, for  $\Theta_1$ , the Lipschitz condition is achieved. Likewise, the Lipschitz condition for  $\Theta_i$  for  $i = 2, \dots, 5$  also holds.

With the help of above concept, one can write

$$\begin{aligned} S^\circ(t) &= S^\circ(0) + \frac{1-\nu}{\mathcal{M}(\nu)} \Theta_1(t, S^\circ) \\ &+ \frac{\nu}{\mathcal{M}(\nu)\Gamma(\nu)} \int_0^t [(t-\zeta)^{\nu-1}] \Theta_1(t, S^\circ) d\zeta. \end{aligned} \quad (11)$$

We can write the above formula as

$$\begin{aligned} S_n^\circ(t) &= S^\circ(0) + \frac{1-\nu}{\mathcal{M}(\nu)} \Theta_1(t, S_{n-1}^\circ) \\ &+ \frac{\nu}{\mathcal{M}(\nu)\Gamma(\nu)} \int_0^t [(t-\zeta)^{\nu-1}] \Theta_1(t, S_{n-1}^\circ) d\zeta. \end{aligned} \quad (12)$$

$S(0) = S_0^\circ$  is an initial condition, and the terms following in order of difference are defined as follows:

$$\begin{aligned} \Lambda_n &= S_n^\circ(t) - S_{n-1}^\circ(t) = \frac{1-\nu}{\mathcal{M}(\nu)} (\Theta_1(t, S_{n-1}^\circ) - \Theta_1(t, S_{n-2}^\circ)) \\ &+ \frac{\nu}{\mathcal{M}(\nu)\Gamma(\nu)} \int_0^t [(t-\zeta)^{\nu-1}] (\Theta_1(t, S_{n-1}^\circ) - \Theta_1(t, S_{n-2}^\circ)) d\zeta. \end{aligned} \quad (13)$$

We get

$$S_n^\circ(t) = \sum_{i=0}^n \Lambda_{1i}(t). \quad (14)$$

Also, we define

$$S_{1-1}^\circ(0) = 0. \quad (15)$$

As a result, we get

$$\Lambda_n \leq \frac{1-\nu}{\mathcal{M}(\nu)} \beta_1 \Lambda_n + \frac{\beta_1 \nu}{\mathcal{M}(\nu)\Gamma(\nu)} \int_0^t \Lambda_{1, n-1}(\zeta) (t-\zeta)^{\nu-1} d\zeta, \quad (16)$$

where  $(\beta_1, \beta_2, \beta_3, \dots, \beta_5) \in (0, 1)^5$ . The existence of the solution is assured by using these results.

**Theorem 4.** If there exists  $\tau_0$  in the considered model, then its solution exists such that

$$\frac{1-\nu}{\mathcal{M}(\nu)} \beta_1 + \frac{\tau_0^\nu \beta_1}{\mathcal{M}(\nu)\Gamma(\nu)} < 1. \quad (17)$$

*Proof.* Let us suppose that the bounded functions exist in the considered system; so, one can obtain

$$\Lambda_n \leq S^\circ(0) \left[ \frac{1-\nu}{\mathcal{M}(\nu)} \beta_1 + \frac{\tau_0^\nu \beta_1}{\mathcal{M}(\nu)\Gamma(\nu)} \right]^n. \quad (18)$$

To express (13) as a solution of (22), we assume that

$$S^\circ(t) - S^\circ(0) = S_n^\circ(t) - U_{1_n}(0). \quad (19)$$

We conclude

$$U_{1_n} \leq \left[ \frac{1-\nu}{\mathcal{M}(\nu)} + \frac{\tau^\nu}{\mathcal{M}(\nu)\Gamma(\nu)} \right]^{n-1} \beta_1^{n-1}, \quad (20)$$

for  $\tau = \tau_0$ .

$$U_{1_n} \leq \left[ \frac{1-\nu}{\mathcal{M}(\nu)} + \frac{\tau_0^\nu}{\mathcal{M}(\nu)\Gamma(\nu)} \right]^{n-1} \beta_1^{n-1}. \quad (21)$$

By applying limit, we have

$$U_{1_n}(t) \longrightarrow \infty. \quad (22)$$

By following the same process, we get

$$U_{i_n}(t) \longrightarrow \infty, \quad (23)$$

for  $i = 1, 2, \dots, 5$ . □

**Theorem 5.** *The considered model has a unique solution if*

$$\left[ 1 - \frac{1-\nu}{\mathcal{M}(\nu)} \beta_1 + \frac{\tau^\nu \beta_1}{\mathcal{M}(\nu)\Gamma(\nu)} \right] > 0. \quad (24)$$

### 4. Proof

We suppose that the model has another solution, that is,  $S$

$$\begin{aligned} \mathcal{S}^\circ(t) - \mathcal{S}_1^\circ(t) &= \frac{1-\nu}{\mathcal{M}(\nu)} (\Theta_1(t, \mathcal{S}^\circ - \Theta_1(t, \mathcal{S}_1^\circ)) \\ &+ \frac{\nu}{\mathcal{M}(\nu)\Gamma(\nu)} \int_0^t [(t-\zeta)^{\nu-1}] (\Theta_1(t, \mathcal{S}^\circ \\ &- \Theta_1(t, \mathcal{S}_1^\circ)) d\zeta. \end{aligned} \quad (25)$$

By the properties of norm, the following inequality is obtained:

$$\mathcal{S}^\circ(t) - \mathcal{S}_1^\circ(t) \left[ 1 - \frac{1-\nu}{\mathcal{M}(\nu)} \beta_1 + \frac{\tau^\nu \beta_1}{\mathcal{M}(\nu)\Gamma(\nu)} \right] \leq 0. \quad (26)$$

If condition of (19) is satisfied, then

$$\mathcal{S}^\circ(t) - \mathcal{S}_1^\circ(t) = 0. \quad (27)$$

Clearly, one can see that

$$\mathcal{S}^\circ(t) - \mathcal{S}_1^\circ(t). \quad (28)$$

For the other components of the model, one can follow the same pattern.

### 5. Problem Formulation

With the  $\mathcal{ABC}$  fractional derivative, we assume the initial-value problem

$${}_0^{\mathcal{ABC}} D_\tau^\nu g(\tau) = f(\tau, g(\tau)). \quad (29)$$

$\mathcal{ABC}$ -PIR ( $\mathcal{BC}$  fractional product integral rule) is given in [24]:

$$g_j = g_0 + \frac{\nu h^\nu}{\mathcal{M}(\nu)} \left( \nu_j f(\tau_0, g_0) + \sum_{i=1}^n \xi_{j-i} f(\tau_i, g_i) \right), \quad (30)$$

where

$$\nu_j = \frac{(j-1)^{\nu+1} - j^\nu(j-\nu-1)}{\Gamma(\nu+2)}, \quad (31)$$

and  $\xi_k$ :

$$\begin{aligned} \xi_k &= \frac{1}{\Gamma(\nu+2)} + \frac{1-\nu}{\nu h h^\nu}, \text{ for } k=0, \\ \xi_k &= \frac{(k-1)^{\nu+1} - 2k^{\nu+1} + (k+1)^{\nu+1}}{\Gamma(\nu+2)}. \text{ for } k=1, 2, \dots, j-1. \end{aligned} \quad (32)$$

By using Eq. (21), we get

$$\begin{aligned} \mathcal{S}_n^\circ &= \mathcal{S}_0^\circ + \frac{\nu h^\nu}{\mathcal{M}(\nu)} [a_j z_1(t_0, \mathcal{S}_0^\circ, \mathcal{V}_0^\circ, \mathcal{E}_0^\circ, \mathcal{F}_0^\circ, \mathcal{R}_0^\circ, \\ &+ \sum_{i=1}^j \xi_{j-i} z_1(t_i, \mathcal{S}_i^\circ, \mathcal{V}_i^\circ, \mathcal{E}_i^\circ, \mathcal{F}_i^\circ, \mathcal{R}_i^\circ)]. \end{aligned} \quad (33)$$

For the remaining equations, we adopt the same pattern as we did above, and we get

$$\begin{aligned} \mathcal{V}_n^\circ &= \mathcal{V}_0^\circ + \frac{\nu h^\nu}{\mathcal{M}(\nu)} [a_j z_2(t_0, \mathcal{S}_0^\circ, \mathcal{V}_0^\circ, \mathcal{E}_0^\circ, \mathcal{F}_0^\circ, \mathcal{R}_0^\circ, \\ &+ \sum_{i=1}^j \xi_{j-i} z_2(t_i, \mathcal{S}_i^\circ, \mathcal{V}_i^\circ, \mathcal{E}_i^\circ, \mathcal{F}_i^\circ, \mathcal{R}_i^\circ), \\ \mathcal{E}_n^\circ &= \mathcal{E}_0^\circ + \frac{\nu h^\nu}{\mathcal{M}(\nu)} [a_j z_3(t_0, \mathcal{S}_0^\circ, \mathcal{V}_0^\circ, \mathcal{E}_0^\circ, \mathcal{F}_0^\circ, \mathcal{R}_0^\circ, \\ &+ \sum_{i=1}^j \xi_{j-i} z_3(t_i, \mathcal{S}_i^\circ, \mathcal{V}_i^\circ, \mathcal{E}_i^\circ, \mathcal{I}_i^\circ, \mathcal{R}_i^\circ), \\ \mathcal{F}_n^\circ &= \mathcal{F}_0^\circ + \frac{\nu h^\nu}{\mathcal{M}(\nu)} [a_j z_4(t_0, \mathcal{S}_0^\circ, \mathcal{V}_0^\circ, \mathcal{E}_0^\circ, \mathcal{F}_0^\circ, \mathcal{R}_0^\circ, \\ &+ \sum_{i=1}^j \xi_{j-i} z_4(t_i, \mathcal{S}_i^\circ, \mathcal{V}_i^\circ, \mathcal{E}_i^\circ, \mathcal{F}_i^\circ, \mathcal{R}_i^\circ), \\ \mathcal{R}_n^\circ &= \mathcal{R}_0^\circ + \frac{\nu h^\nu}{\mathcal{M}(\nu)} [a_j z_5(t_0, \mathcal{S}_0^\circ, \mathcal{V}_0^\circ, \mathcal{E}_0^\circ, \mathcal{F}_0^\circ, \mathcal{R}_0^\circ, \\ &+ \sum_{i=1}^j \xi_{j-i} z_5(t_i, \mathcal{S}_i^\circ, \mathcal{V}_i^\circ, \mathcal{E}_i^\circ, \mathcal{F}_i^\circ, \mathcal{R}_i^\circ)]. \end{aligned} \quad (34)$$

## 6. Numerical Simulation

This study's primary goal was to evaluate how vaccination strategies affected the dynamics of disease transmission. Graphs are depicting the parametric variation with regard to various variables that are offered here to support the analytical conclusions. Since the majority of the parameters are not immediately available, it is deemed appropriate to estimate solely for the purpose of illustrative purposes to show how the model would react in various real-world scenarios as given in Table 2. The Euler method has been used for numerical simulation of the problem [22].

Figure 2 depicts simulations with various vaccination rates for neonates. As the outbreak develops later, the vaccination drive begins to have an impact, reducing the 160 overall population of individuals who are susceptible; this reduction in susceptible people will naturally result in a reduction in the number of sick people, controlling the disease outbreak.

Figure 3 depicts simulations with various vaccination rates for neonates. As the outbreak spreads later, the vaccination drive begins to have an impact, reducing the overall number of infected people; this reduction in sick people will automatically result in the elimination of VZV from the neighborhood. Although a newborn-focused vaccination effort is ideal for a nation's future, it does not immediately result in the illness being eradicated. Random mass vaccination must be used to have immediate results, which necessitates immunizing a sizeable portion of the population.

Figure 4 shows that when vaccination rates for susceptible adults rise, the fraction of susceptible people tends to decline. As a result, there are fewer people who become ill, which lowers the incidence of chickenpox.

Figure 5 shows that there is a small decline in the compartment of susceptible people when the double dose population increases. This is because susceptible people are not necessarily those who receive the second dose; instead, they only receive second dose two when they are already vaccinated. This circumstance is what caused the slight decrease in the susceptible population. In order to reduce the disease, this method generally has a minor yet considerable effect.

Figure 6 shows that there are more recovered people as newborn vaccination rates rise. Conversely, when newborns are not vaccinated, there are more recovered people. This may be because the sick people have natural immunity, and a corresponding decline may be caused by immunity loss that actually wane with time. It can be seen in Figure 6 that there is a noticeable rise in the number of recovered people when almost a half of neonates receive vaccinations. However, with the passage of time, one can observe a fall in the compartment of recovered persons. The results are consistent with our hypothesis that the effectiveness of the first dosage of vaccine waned over the period of time, necessitating the need for the second vaccine to enhance vaccination rates. When vaccination covers the population 100 percent, the slope of the graph increases, and then nearly remains constant after reaching the maximum point, indicating that the 190 infection can be completely eradicated from the community.

TABLE 2: Parameters' values.

Parameters	Value
$\kappa_1$	0.7
$\kappa_2$	0.8
$\varsigma$	0.5
$\rho$	0.45
$\alpha$	0.36
$\delta_2$	0.7
$\chi_2$	0.6
$\chi_1$	0.3
$\epsilon$	0.2

From Figure 1, it is evident that suspected population increases with decrease in the fractional order and two-scale dimension. And it is the lowest when the problem reaches the order 1. The case is opposite for vaccinated population and exposed population, that is, compartments  $V$  and  $E$  reach its maximum value for the lowest two-scale dimension and fractional order as shown in Figures 2 and 3. Recovered population increases exponentially for the lowest value of fractal dimension.

## 7. Results and Discussion

In this work, a noninteger order model of SIVER models with two viruses is formulated through ABC operator. The existence theory is provided with the help of fixed-point theorem. We used an iterative strategy to find a unique solution to the hypothesized fractional SIRS model with two viruses. Numerical findings are produced for various values of the fractional parameters. As a result, the government must take steps to educate people in rural regions, provide vaccinations, and provide proper treatment in hospitals and other health care facilities. Because we applied the concept of two-scale with Atangana-Baleanu fractional derivatives, the current study will be more useful than prior studies. Our findings predicted that the outcomes of fractional derivative are more precious than the ordinary system.

*7.1. Effect of  $\kappa_1$ .* When the entire adult population received the first dosage of the vaccine, the number of susceptible and infectious people quickly decreased (in the case of  $\kappa_1 = 1$ ). This indicates that the first dose of vaccination had a major impact. Figure 4 demonstrates that as the proportion of adults who are susceptible to the disease is increased by vaccination, the proportion of susceptible adults tends to decrease. As a result, there are fewer sick people and, consequently, fewer cases of chicken pox. As the effects of the initial dose started to wear off, this reduction in the proportion of susceptible and infectious shifted. The entire population contracted the disease, which caused it to reappear. If this tendency is not reversed soon, it could cause future outbreaks of the illness, which could eventually become endemic. This calls for the second dosage of the vaccine to be administered.

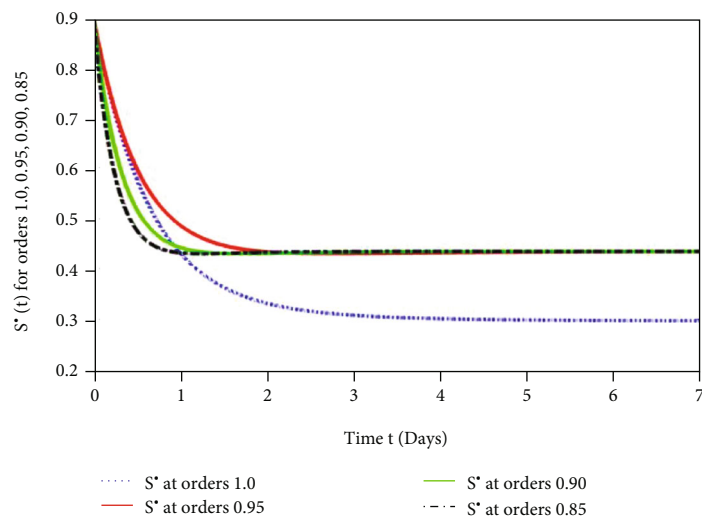


FIGURE 2: Susceptible population.

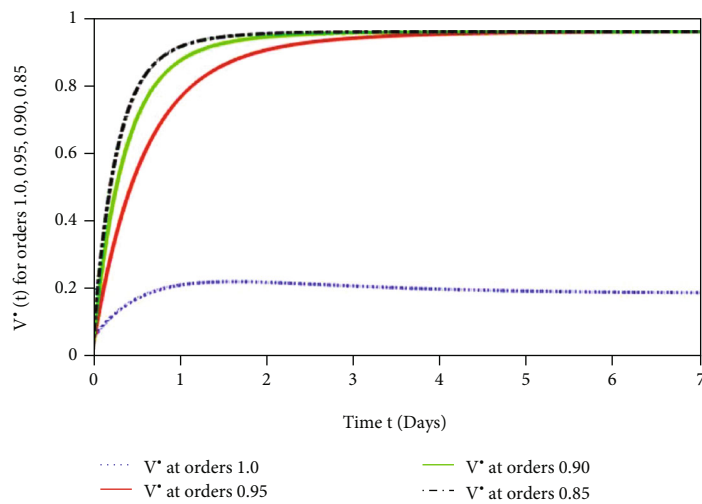


FIGURE 3: Vaccinated population.

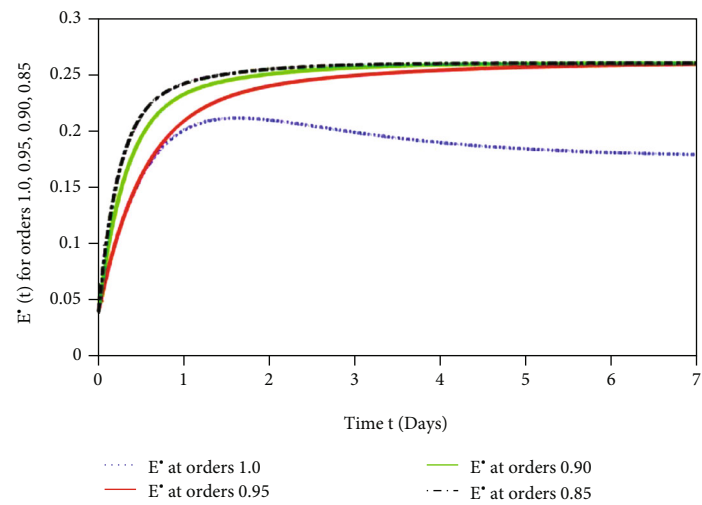


FIGURE 4: Exposed population.

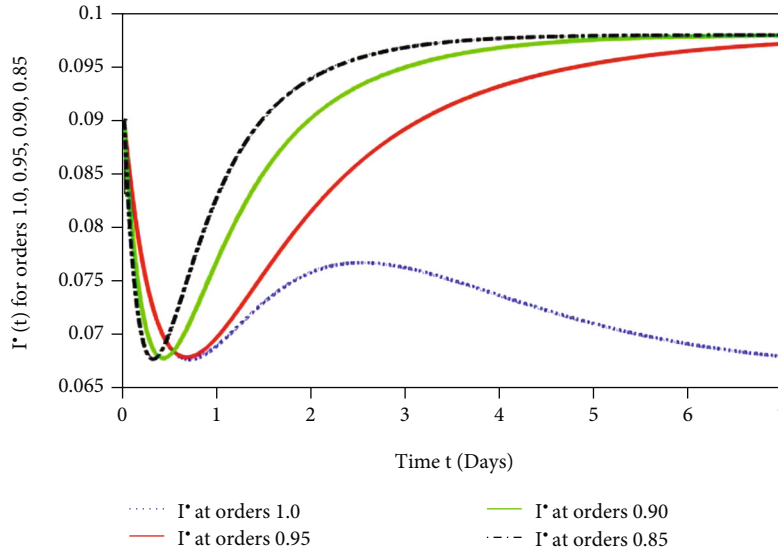


FIGURE 5: Infected population.

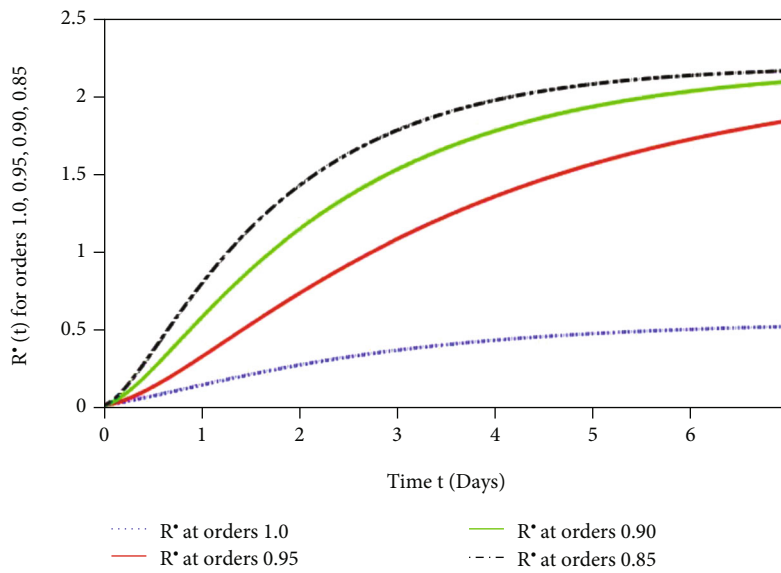


FIGURE 6: Recovered population.

7.2. *Effect of  $\kappa_2$ .* Figure 3 shows that there is a slight but significant decrease in the fraction of sensitive individuals as dosage two coverage among humans increases. This is because the individuals that received the second dose are not directly connected to susceptible persons. Humans who are susceptible will only take dosage two if they have already gotten dose one; otherwise, they will not. Due to the possibility that these individuals may be newborns or recruits, who would not or would have a minimal impact on the population of susceptible, this circumstance led to a minor fall in the insusceptible population even though more people received dosage two of the vaccination. Therefore, this practice generally has a minor but considerable effect in lowering the sickness.

7.3. *Recovery Rate.* Figure 6 demonstrates how the quantity of recovered people rises as infant immunization coverage does. Additionally, it may be observed that when neonates are not immunized, the proportion of the population that recovers gradually decreases, possibly as a result of the sick people’s innate immunity. Immunity loss, which worsens over time, may be the cause of this decline in the recovery percentage. The grey line in Figure 6’s graph shows that when 50 percent of newborns receive immunizations, there is a discernible increase in the number of recovered humans.

Numerous studies have used the ABC fractional operator to depict different sickness models, and the results support the validity of the concept. We investigated  $\mathcal{VEV}$  using the same methodology in order to come up with a

workable solution. The graphical findings were obtained using MATLAB 2020. We draw the conclusion from these graphical results that one can achieve more accurate results and gain a better understanding of both an enzyme reaction equation system and real-world problems in science and engineering by using this new notion of the two-scale and ABC fractional operator.

## 8. Concluding Remarks

We used a new fractional ABC derivative in arithmetic to solve the problem under consideration. To incorporate the scale effect in the model under consideration, the concept of two-scale fractal dimension has been taken into consideration. The results of fractional order are demonstrated by numerical simulation. The outcomes demonstrate the effectiveness of the fractional derivative operator, integral operators, and two-scale transform in ABC approach. So, we can conclude that the strategy under consideration is effective. The nature of a large class of nonlinear fractional-order mathematical models in engineering and research can be studied using this method.

## 9. Future Recommendation

In the current research era, fractal theory and fractional calculus have become particularly popular topics. A new step forward in understanding natural fractals and hierarchical structures is the two-scale fractal theory. The idea that all physical laws are scale-dependent and that each law is only true on the specified scale above which there are stochastic features is projected by the two-scale dimension. To address a specific issue, two observational scales can be chosen. Three scales may be proposed in the future for computations that are more accurate.

To solve the mathematical model of varicella-zoster virus, two-scale dimension has been used. In future, fractal derivative, distance, velocity, and two-scale transform can be applied. To strengthen the mathematical underpinnings of two-scale fractal theory, additional mathematical definitions may be added in the future.

## Data Availability

All the data are available within the article.

## Conflicts of Interest

The authors declare that they have no competing of interest.

## References

- [1] M. Almuneef, Z. A. Memish, H. H. Balkhy, B. Alotaibi, and M. Helmy, "Chickenpox complications in Saudi Arabia: is it time for routine varicella vaccination," *275 International journal of infectious diseases*, vol. 10, no. 2, pp. 156–161, 2006.
- [2] A. A. Gershon, "Varicella-zoster virus infections," *Pediatrics in Review*, vol. 29, no. 1, 2008.
- [3] L. Gregorakos, P. Myrianthefs, N. Markou, D. Chroni, and E. Sakagianni, "Severity of illness and outcome in adult patients with primary varicella pneumonia," *Respiration*, vol. 69, no. 4, pp. 330–334, 2002.
- [4] C. K. Fairley and E. Miller, "Varicella-zoster virus epidemiology—a changing scene," *Journal of infectious diseases*, vol. 174, Supplement 3, pp. S314–S319, 1996.
- [5] B. W. Lee, "Review of varicella zoster seroepidemiology in India and South-East Asia," *Tropical medicine & international health: TM & IH*, vol. 3, no. 11, pp. 886–890, 1998.
- [6] C. Cattani, H. M. Srivastava, and X. J. Yang, *Fractional dynamics*, Walter de Gruyter GmbH & Co KG, 2015.
- [7] K. M. Kolwankar and A. D. Gangal, *Local fractional calculus: a calculus for fractal space-time*, InFractals, Springer, London, 1999.
- [8] A. Atangana, "Fractal-fractional differentiation and integration: connecting fractal calculus and fractional calculus to predict complex system," *Chaos, solitons & fractals*, vol. 102, pp. 396–406, 2017.
- [9] A. Atangana and S. Qureshi, "Modeling attractors of chaotic dynamical systems with fractal-fractional operators," *Chaos, solitons & fractals*, vol. 123, pp. 320–337, 2019.
- [10] Q. T. Ain and J.-H. He, "On two-scale dimension and its applications," *Thermal Science*, vol. 23, no. 3 Part B, pp. 1707–1712, 2019.
- [11] J.-H. He and Q.-T. Ain, "New promises and future challenges of fractal calculus: from two-scale thermodynamics to fractal variational principle," *Thermal Science*, vol. 24, no. 2 Part A, pp. 659–681, 2020.
- [12] J.-H. He, G. M. Moatimid, and M. H. Zekry, *Forced Nonlinear Oscillator in a Fractal Space*, *Facta Universitatis*, Series: Mechanical Engineering, 2022.
- [13] A. Elisha, T. Aboiyar, and A. R. Kimbir, "Mathematical analysis of varicella zoster virus model," *Applied and Computational Mathematics*, vol. 6, no. 2, 2021.
- [14] F. Haq, M. Shahzad, S. Muhammad, H. A. Wahab, and G. ur Rahman, "Numerical analysis of fractional order epidemic model of childhood diseases," *Discrete Dynamics in Nature and Society*, vol. 2017, Article ID 4057089, 7 pages, 2017.
- [15] I. Ameen, M. Hidan, Z. Mostefaoui, and H. M. Ali, "Fractional optimal control with fish consumption to prevent the risk of coronary heart disease," *Complexity*, vol. 2020, Article ID 9823753, 13 pages, 2020.
- [16] A. Ullah, T. Abdeljawad, S. Ahmad, and K. Shah, "Study of a fractional-order epidemic model of childhood diseases," *Journal of Function Spaces*, vol. 2020, Article ID 5895310, 8 pages, 2020.
- [17] H. M. Alshehri and A. Khan, "A fractional order hepatitis C mathematical model with Mittag-Leffler kernel," *Journal of Function Spaces*, vol. 2021, Article ID 2524027, 10 pages, 2021.
- [18] M. Helikumi, G. Eustace, and S. Mushayabasa, "Dynamics of a fractional-order chikungunya model with asymptomatic infectious class," *Computational and Mathematical Methods in Medicine*, vol. 2022, Article ID 5118382, 19 pages, 2022.
- [19] H. Mohammadi, M. K. Kaabar, J. Alzabut, A. Selvam, and S. Rezapour, "A complete model of Crimean-Congo hemorrhagic fever (CCHF) transmission cycle with nonlocal fractional derivative," *Journal of Function Spaces*, vol. 2021, Article ID 1273405, 12 pages, 2021.
- [20] A. Harir, S. Melliani, H. El Harfi, and L. S. Chadli, "Variational iteration method and differential transformation method for solving the SEIR epidemic model," *International Journal of*

*Differential Equations.*, vol. 2020, Article ID 3521936, 7 pages, 2020.

- [21] A. Elias-Zuniga, "On two-scale dimension and its application for deriving a new analytical solution for the fractal DUFFINGS equation," *Fractals*, vol. 30, no. 3, 2022.
- [22] H. Yuan, "Some properties of numerical solutions for semi-linear stochastic delay differential equations driven by G-Brownian motion," *Mathematical Problems in Engineering.*, vol. 2021, Article ID 1835490, 26 pages, 2021.
- [23] A. Din, Y. Li, F. M. Khan, Z. U. Khan, and P. Liu, "On analysis of fractional order mathematical model of hepatitis B using Atangana Baleanu Caputo (ABC) derivative," *Fractals*, vol. 30, no. 1, 2022.
- [24] A. Din, "The stochastic bifurcation analysis and stochastic delayed optimal control for epidemic model with general incidence function," *Journal of Nonlinear Science.*, vol. 31, no. 12, article 123101, 2021.